# *Supporting Information*

## Poly(3-hexylthiophene)-block-poly(tetrabutylammonium-4-styrenesulfonate) Block Copolymer Micelles for the Synthesis of Polymer Semiconductor Nanocomposites

Paul M. Reichstein, [†] Johannes C. Brendel, [†,§] Markus Drechsler, [‡] Mukundan Thelakkat*,[†,‡]

[†] Applied Functional Polymers, Macromolecular Chemistry I and [‡] Bavarian Polymer Institute (BPI), University of Bayreuth, Universitätsstr. 30, Bayreuth 95440, Germany

*Corresponding author: mukundan.thelakkat@uni-bayreuth.de

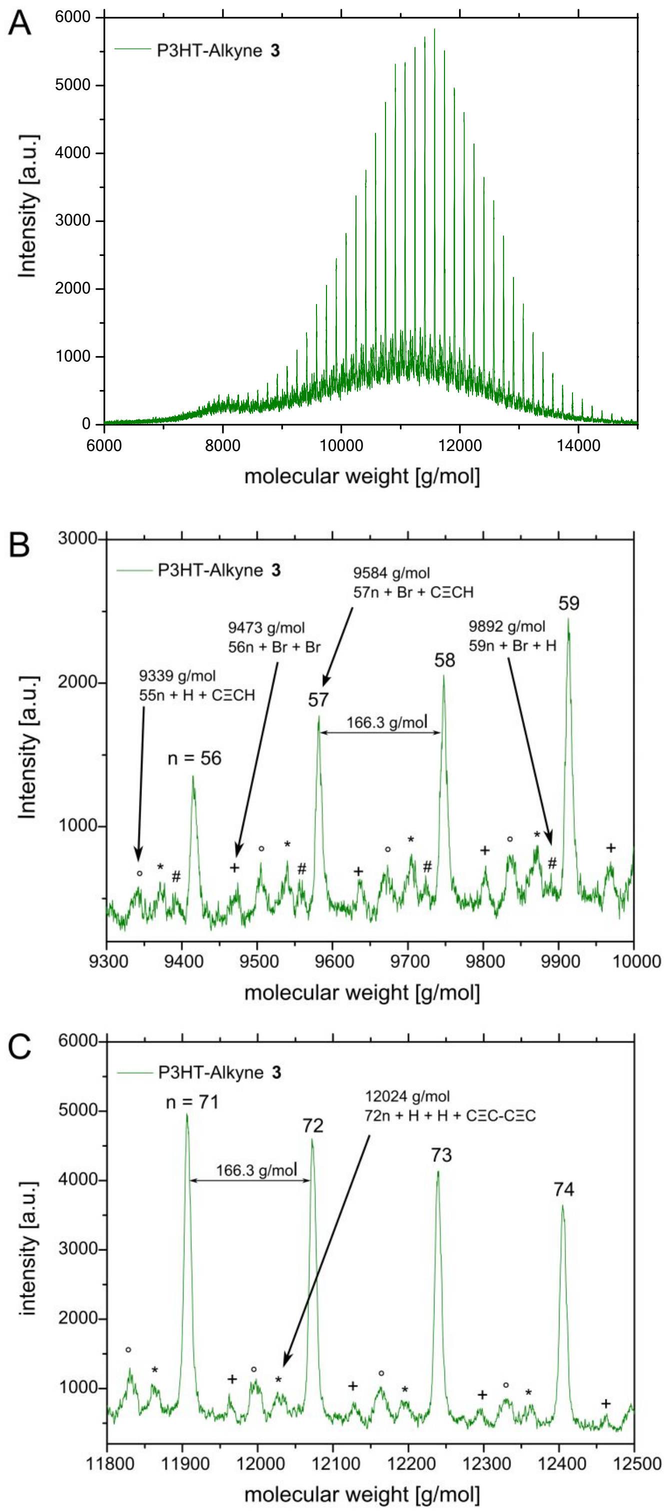


**Figure S1.** MALDI-ToF of P3HT-Alkyne with the whole molecular weight distribution (A) and detailed analysis of signals for polymer chains with 56-59 repeating units (B) and 71-74 repeating units (C).

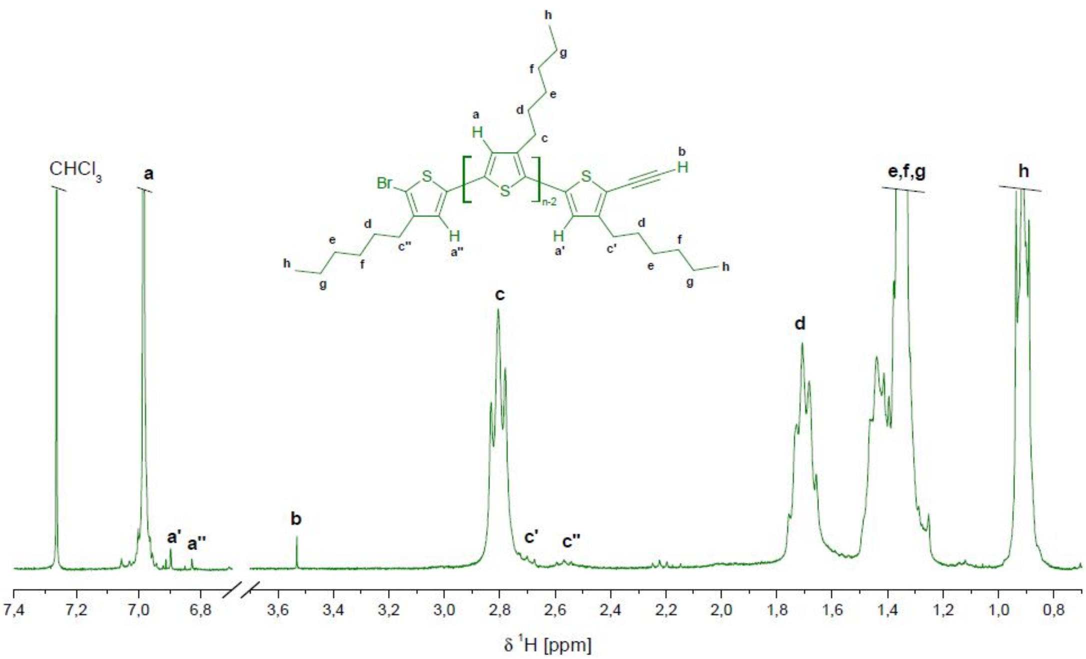


**Figure S2.** $^{1}$H-NMR of P3HT-Alkyne, the signal of the alkyne proton b can be seen at δ = 3.51 ppm.

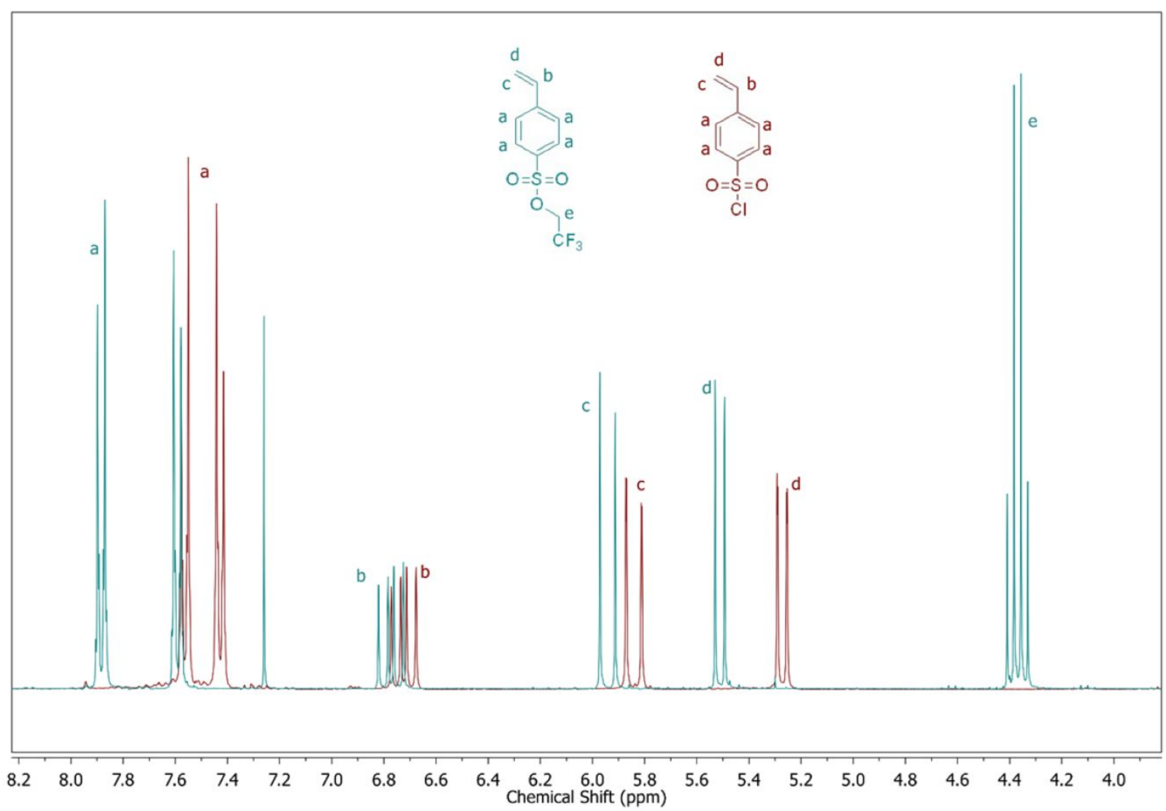


**Figure S3.** $^{1}$H-NMR of 4-vinylbenzene-1-sulfonyl chloride (red) and 2,2,2-trifluoroethyl-4-vinylbenzenesulfonate (green). The overlay of the two spectra shows the complete conversion during the synthesis.

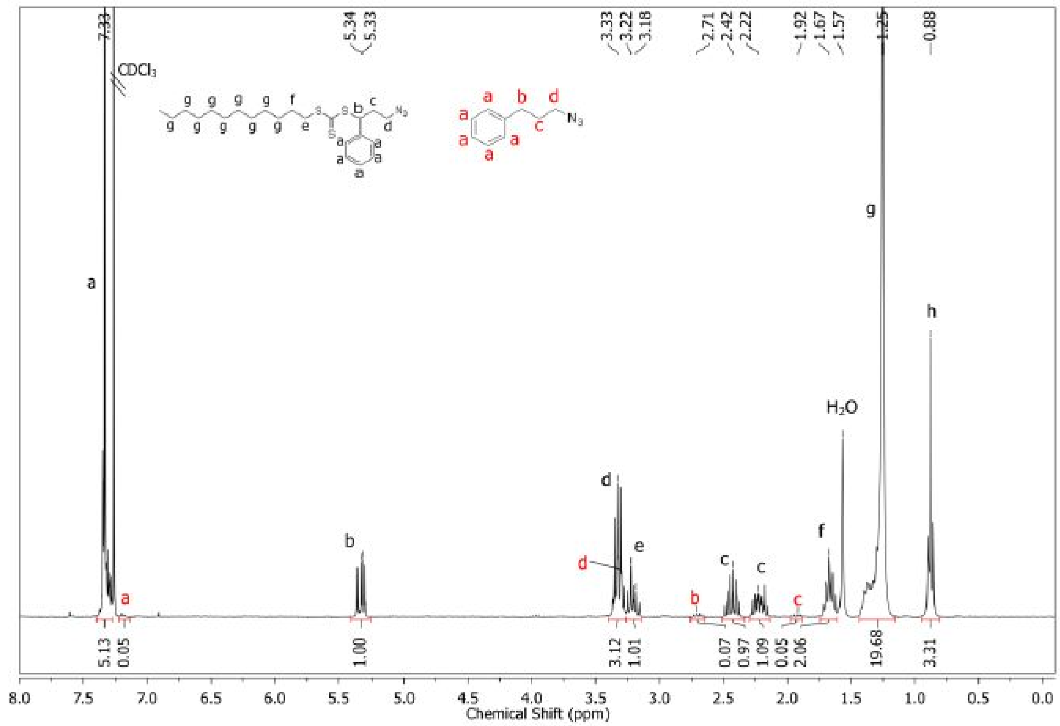


**Figure S4.** [1]H-NMR of 3-azido-1-phenylpropyl dodecyl trithiocarbonate (black) where small impurities (>5 mol-%) of the educt 3-azidopropylbenzene (red) are still present after purification by column chromatography.

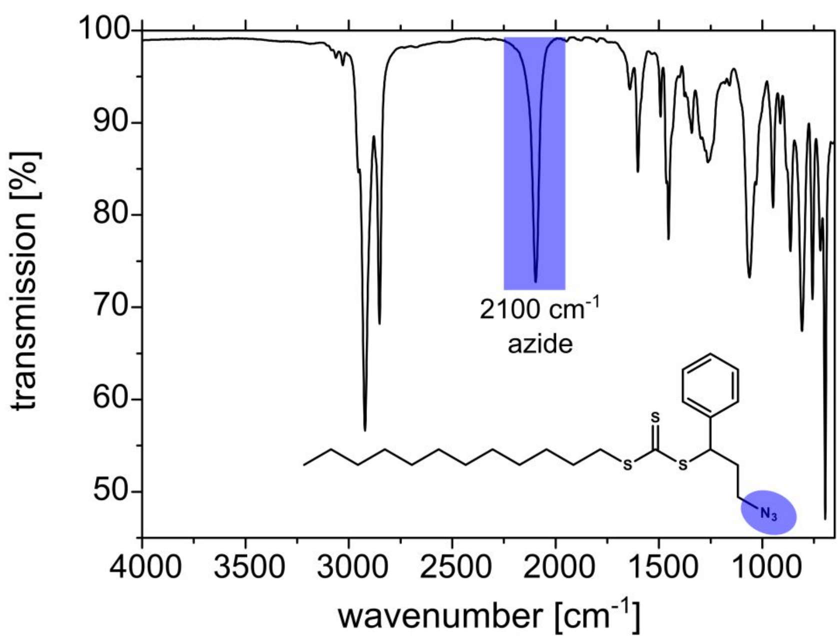


**Figure S5.** FT-IR spectrum of 3-azido-1-phenylpropyl dodecyl trithiocarbonate where the intense azide band is clearly visible at 2100 cm$^{-1}$ and proves the successful synthesis of the clickable RAFT agent.

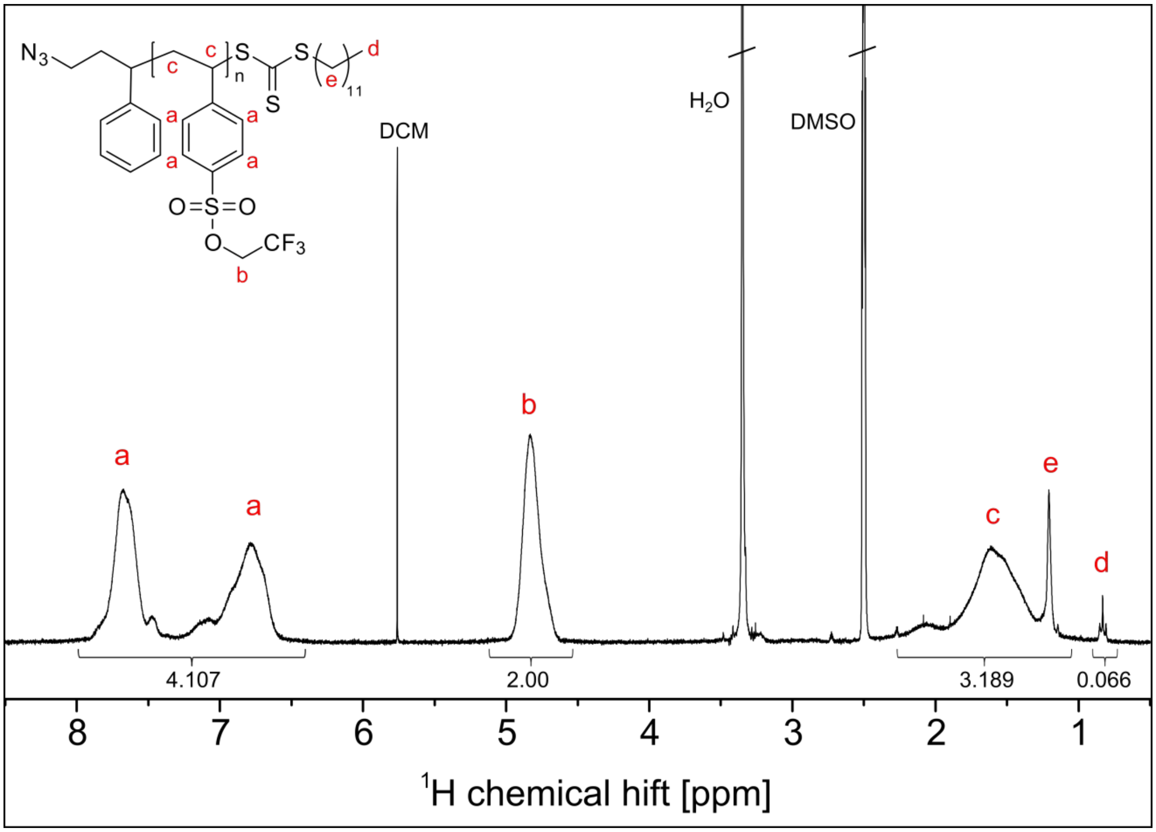


**Figure S6.** $^1$H-NMR of P(SS-$CH_2$-$CF_3$)-$N_3$ measured in d-DMSO. The proton signals next the azide end group cannot be seen, because they are of small intensity and hidden under the backbone signals.

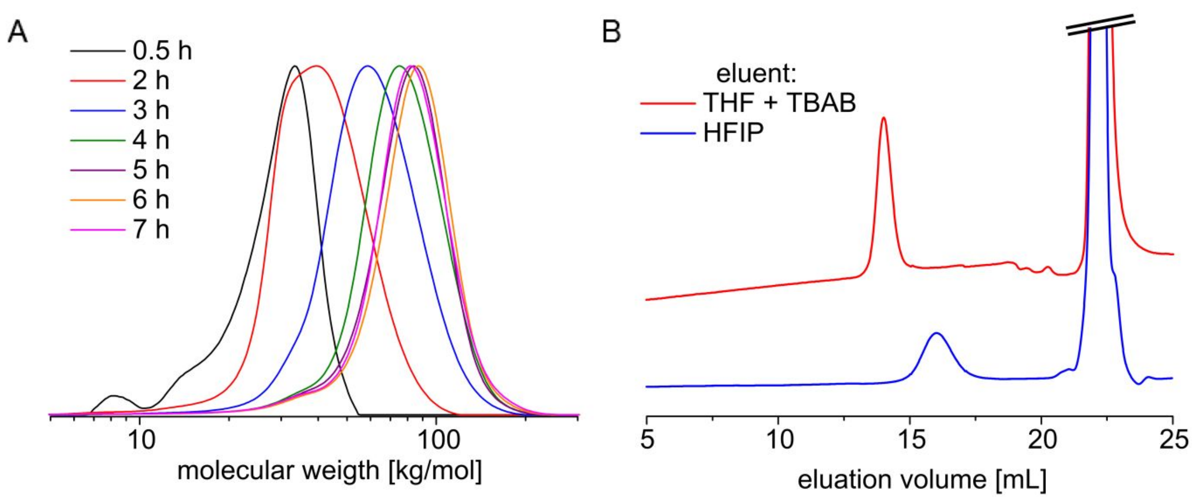


**Figure S7.** (A) Molecular weight distributions of P(SS-$CH_2$-$CF_3$)-$N_3$ during polymerization and (B) comparison of elugrams of P(SS-$CH_2$-$CF_3$)-$N_3$ with the solvents HFIP (toluene as internal standard) and THF + TBAB (o-dichlorobenzene as internal standard).

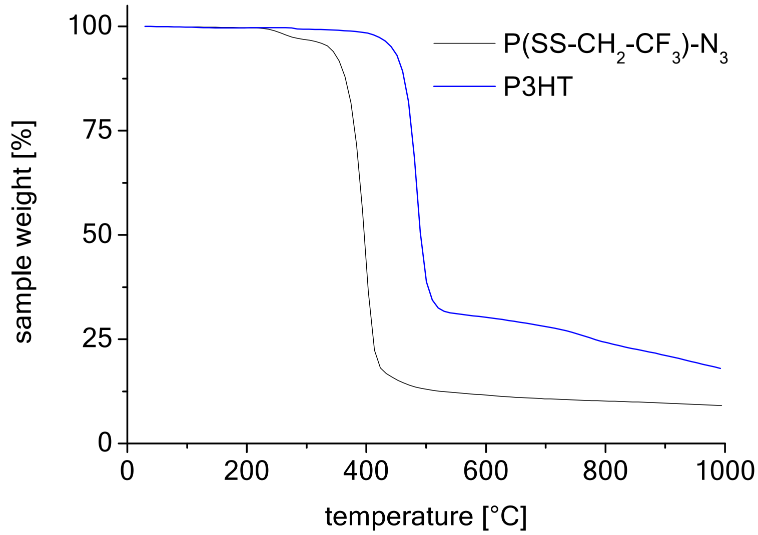


**Figure S8.** TGA analysis of P3HT-Alkyne and P(SS-$CH_2$-$CF_3$)-$N_3$ measured under $N_2$ atmosphere.

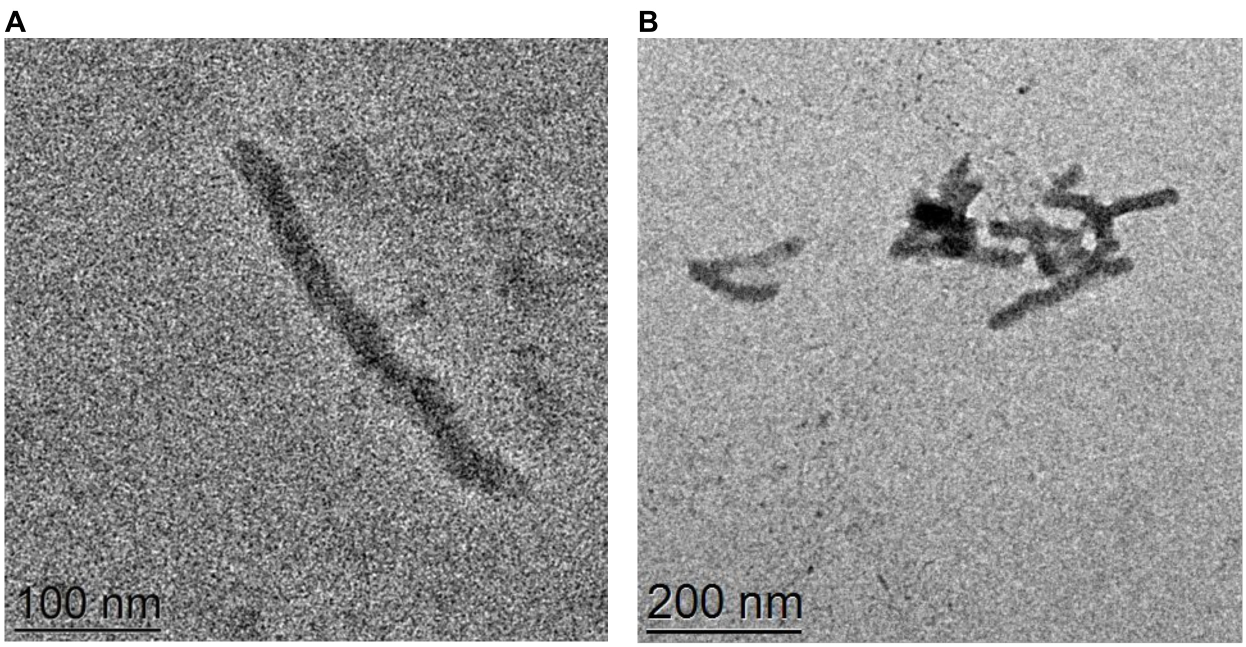


**Figure S9.** TEM images of P3HT-b-$PSS^-$/$TBA^+$ micelles. The micelles have a wormlike structure (A) and branched shapes can be a result of agglomeration during drying (B). Samples were prepared by putting the micelle solution on the TEM-grid and remove the solvent without staining.

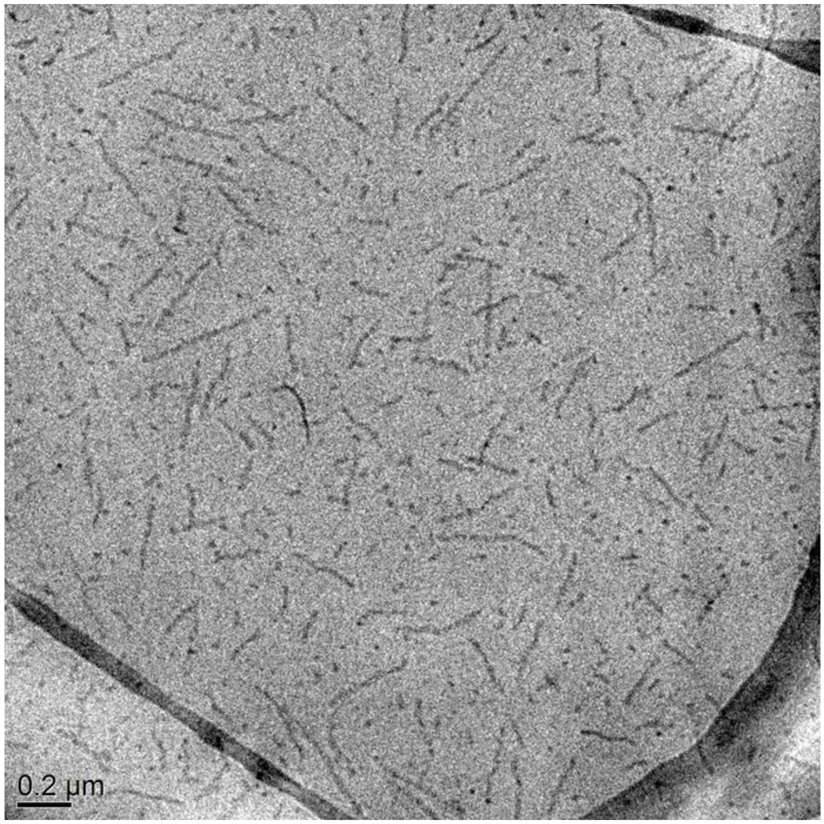


**Figure S10.** cryo-TEM images of P3HT-b-$PSS^-$/$TBA^+$ micelles without staining (overview).

**A** **B**

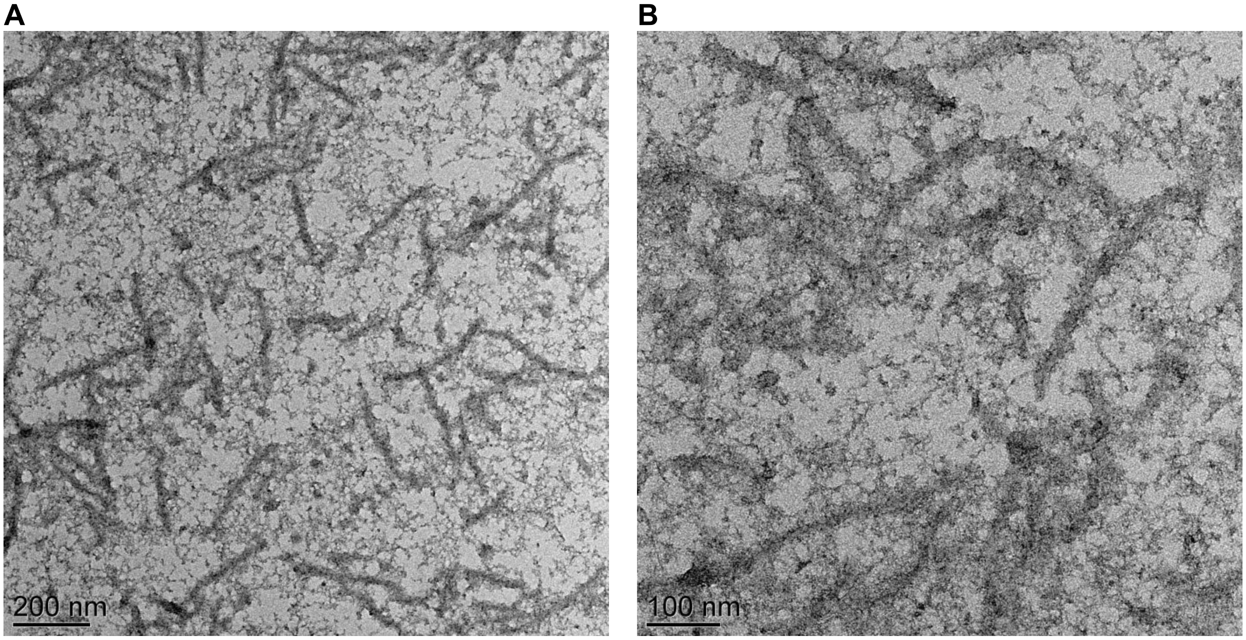


**Figure S11.** TEM images of dried P3HT-b-$PSS^-$/$TBA^+$ + $TiO_2$ nanocomposites without staining.

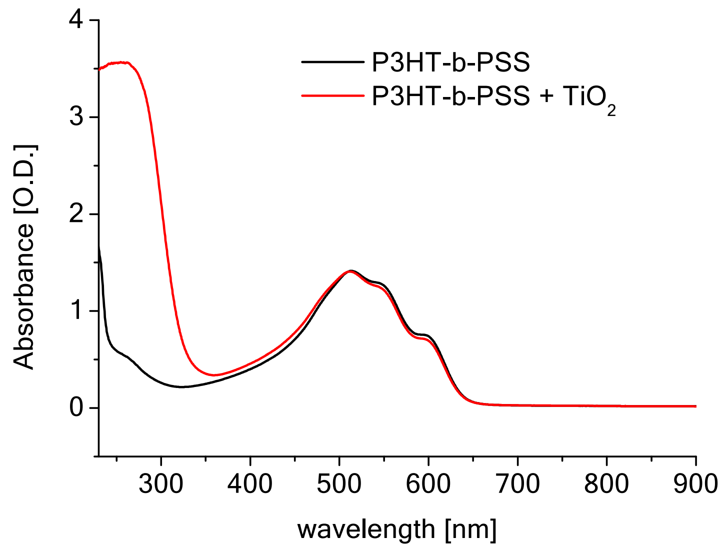


**Figure S12.** UV-vis spectra of P3HT-b-PSS$^-$/TBA$^+$ micelles in water and P3HT-b-PSS$^-$/TBA$^+$ + $TiO_2$ in water.